In situ TEM tensile testing of carbon-linked graphene oxide nanosheets using a MEMS device

2016 Nanotechnology 27 28LT01

(http://iopscience.iop.org/0957-4484/27/28/28LT01)

IOP Publishing

Letters

Nanotechnology

Nanotechnology **27** (2016) 28LT01 (4pp)

doi:10.1088/0957-4484/27/28/28LT01

Letter

In situ TEM tensile testing of carbon-linked graphene oxide nanosheets using a MEMS device

Changhong Cao[1], Jane Y Howe[2,3], Doug Perovic[3,4], Tobin Filleter[1,4] and Yu Sun[1,4]

[1] Department of Mechanical and Industrial Engineering, University of Toronto, Toronto, ON, M5S 3G8, Canada

[2] Hitachi High-Technologies Canada, Inc., Toronto, ON, M9W 6A4, Canada

[3] Department of Materials Science and Engineering, University of Toronto, Toronto, ON, M5S 3E4, Canada

E-mail: Doug.Perovic@utoronto.ca, filleter@mie.utoronto.ca and sun@mie.utoronto.ca

Received 4 May 2016
Accepted for publication 16 May 2016
Published 3 June 2016

Abstract

This paper reports *in situ* transmission electron microscopy (TEM) tensile testing of carbon-linked graphene oxide nanosheets using a monolithic TEM compatible microelectromechanical system device. The set-up allows direct on-chip nanosheet thickness mapping, high resolution electron beam linking of a pre-fractured nanosheet, and mechanical tensile testing of the nanosheet. This technique enables simultaneous mechanical and high energy electron beam characterization of 2D nanomaterials.

Keywords: *in situ* TEM, MEMS, graphene oxide, mechanical property

Introduction

Mechanical properties of low-dimensional nanomaterials, such as carbon nanotubes, graphene, and hexagonal-boron nitride, are of fundamental importance when these nanomaterials are used as building blocks in composites [1, 2], or as key components in electronic devices [3] and energy storage devices [4, 5]. However, mechanical characterization of materials at this length scale is challenging partly due to instrumentation difficulties. For example, commonly used atomic force microscopy based indentation tests are limited to probing local properties of materials [6, 7]. Applying microelectromechanical systems (MEMS) inside electron microscopes can significantly benefit the characterization processes by precisely conducting mechanical measurements under high resolution imaging conditions. For example, the mechanical properties of 1D materials (silicon nanowires) have been characterized using a MEMS device under scanning electron microscope (SEM) [8, 9]. Recently, a MEMS *in situ* SEM technique was also used to measure 2D nanomaterials. The strength of graphene oxide nanosheets was measured as high as 12 GPa, approaching that of monolayer graphene, by using a MEMS device under SEM [10]. Although *in situ* SEM mechanical characterization of 2D materials was demonstrated and the results filled in the gap of mechanical properties of films at the intermediate length scale between monolayer and bulk [11], the imaging resolution of SEM restricted a more detailed characterization of material morphologies. The intrinsic limitations of SEM including imaging resolution and structural characterization motivated the pursuit of *in situ* MEMS characterization under transmission electron microscopy (TEM).

TEM provides significantly higher imaging resolution than SEM and enables controllable electron-induced material modification. For instance, CNTs have been demonstrated to be cross-linked by electron irradiation and mechanically

[4] Authors to whom any correspondence should be addressed.

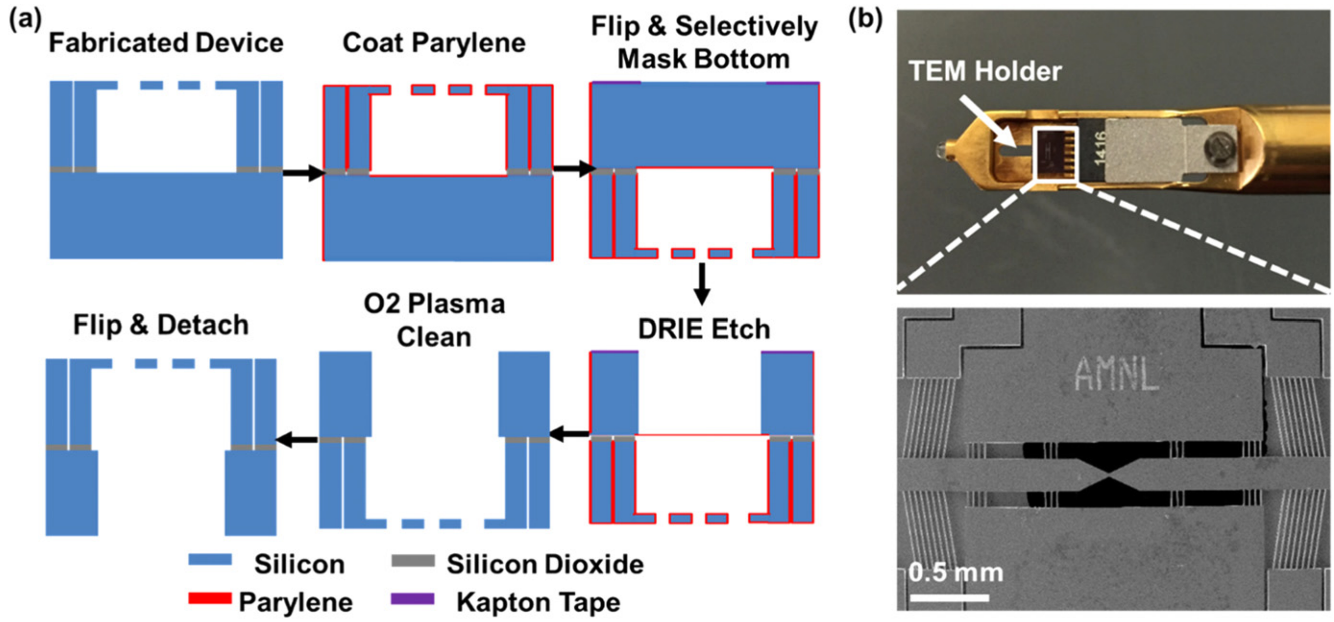

Figure 1. (a) Post processing of SOI-MUMPs fabricated the MEMS tensile testing device to make it TEM compatible. (b) MEMS device was mounted on a custom-built TEM holder to perform tensile testing under TEM imaging.

tested using a MEMS device under TEM. The results showed cross-linked CNTs have significantly higher effective strengths and moduli [12]. However, mechanical characterization of 2D nanomaterials using a monolithic MEMS device under TEM has not yet been reported. This paper reports a TEM compatible monolithic MEMS tensile tester and demonstrates tensile testing of a linked GO nanosheet after carbon linking of a pre-fractured GO nanosheet via electron beam induced deposition. This MEMS device is the first TEM compatible monolithic tensile tester demonstrated to perform mechanical characterization of 2D nanomaterials.

Device design and fabrication

As shown in figure 1, the MEMS device uses V-beam thermal microactuators on both sides of opposite shuttle platforms onto which a GO nanosheet is placed. The device was constructed using a standard SOI-MUMPs process [13]. To allow electrons to transmit through the device for TEM compatibility, a post fabrication process was developed to form a through-window that was etched from the handle layer Si until the bottom of the device Si layer. Due to the lack of a stop layer in the target etching region, protecting existing features from the etching process must be properly done. By coating a 1 μm thick parylene film on the top of the device layer, it acts as a stop layer to prevent over etching of the device layer. Parylene was removed using oxygen plasma after the backside window was created. GO nanosheet was deposited via dropcasting GO solution to bridge the gap of the shuttle on the MEMS device, according to the protocol we developed previously [10]. The MEMS device was then mounted on a custom-built TEM (Hitachi High-Technologies Canada) holder that establishes electrical connections with the MEMS structures. Tensile testing of GO nanosheet was performed by the MEMS device using a Hitachi HF-3300 TEM/STEM/SEM at 100 kV. This TEM has a secondary electron detector on its scanning transmission electron microscopy (STEM) unit which allows simultaneous bright-field and annular dark-field transmitted electron imaging (BF-TEM and ADF-TEM) and secondary electron imaging (SEM).

Carbon linked GO and on-chip thickness mapping

Figure 2 shows scanning transmission electron microscope images of a GO nanosheet with a pre-crack that was used as the starting material. The entire large crack was linked patch by patch by amorphous carbon deposition using a high energy electron beam at 100 KeV with an emission current of 9 nA, as shown in figures 2(b)–(d). Figures 2(e) and (f) show representative high resolution images of the crack before and after carbon linking. The linked GO nanosheet was examined using BF-TEM before tensile testing (figures 2(g) and (h)). Thickness of the linked GO nanosheet was examined on chip by measuring the number of mean free path (MFP) via electron energy loss spectroscopy (EELS) at 100 KeV incident energy, which was then converted to thickness by multiplying the MFP of arc-evaporated carbon film (116 nm) [14] to give an average thickness of 27 $\pm$ 7 nm across the nanosheet (figure 3). The carbon linked region is assumed to have approximately the same thickness to GO nanosheet.

Tensile testing

Figures 4(a)–(d) show images captured during tensile testing of the completely carbon linked GO nanosheet, with an

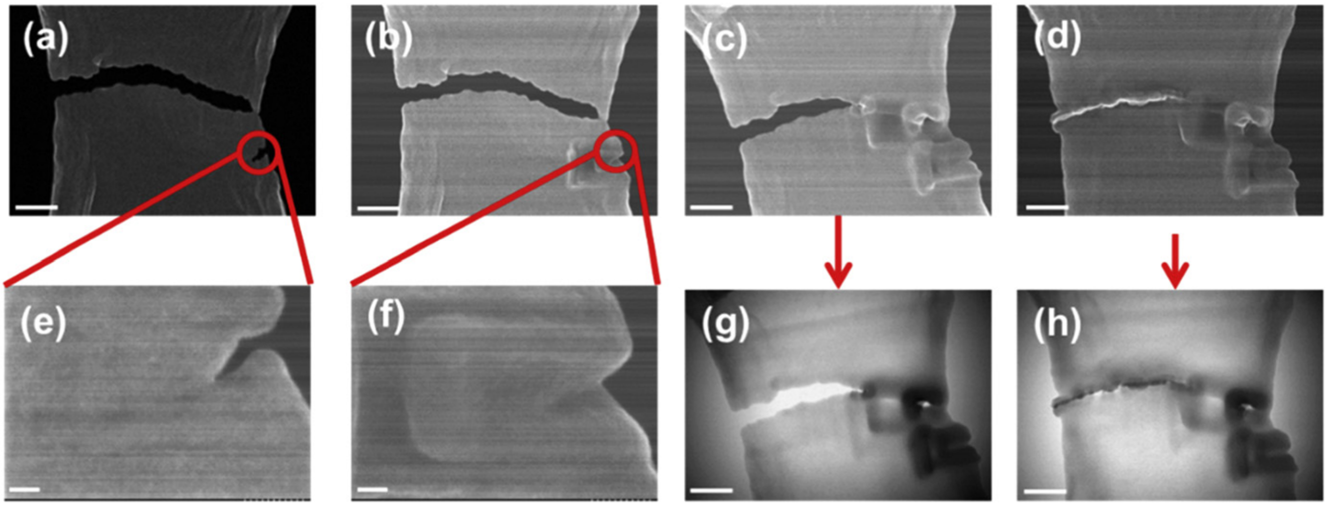

Figure 2. (a)–(d) STEM images of a pre-fractured GO nanosheet. The nanosheet was crosslinked patch by patch by high energy, high resolution electron beam. (Scale bar: 150 nm). (e) and (f) High magnification images of the red-circled regions in (a) and (b) (scale bar: 15 nm). (g) and (h) BF-TEM images of (c) and (d) (scale bar: 150 nm).

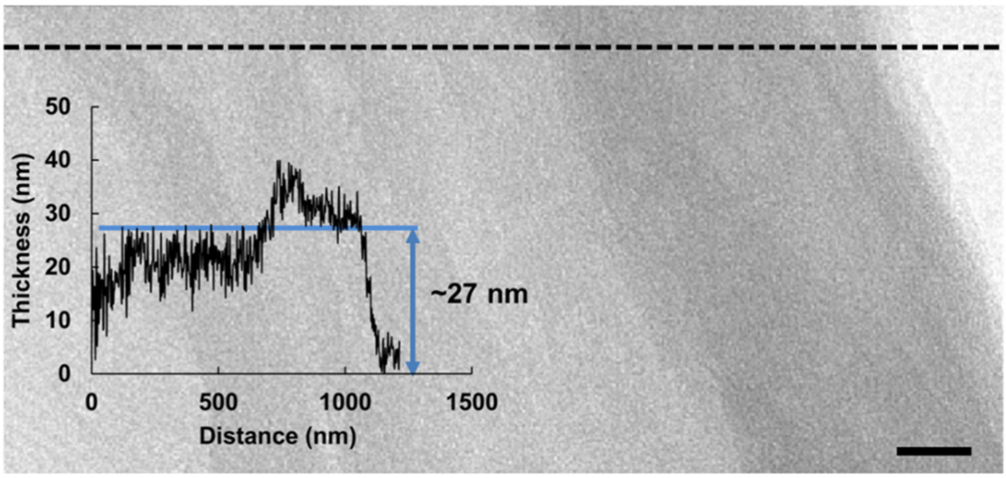

Figure 3. EELS thickness mapping of the GO nanosheet (scale bar: 100 nm); inset: thickness profile of the GO nanosheet along the black dash line.

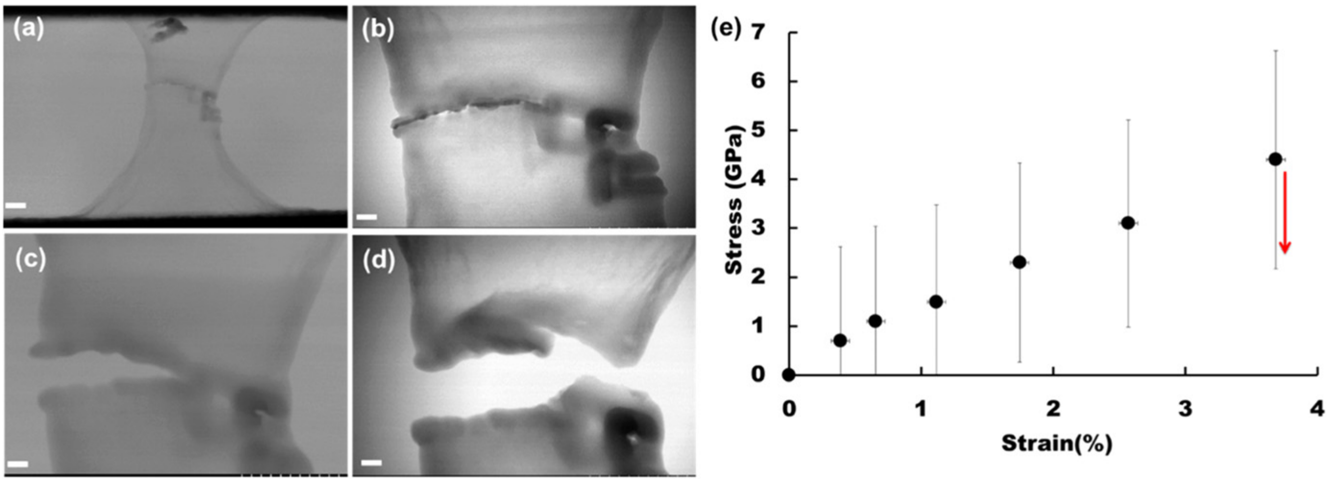

Figure 4. BF-TEM images and mechanical response captured during *in situ* TEM tensile measurement of a crosslinked GO nanosheet. (a) Crosslinked GO nanosheet positioned across the MEMS shuttle, under TEM imaging (scale bar: 100 nm). (b), (c) and (d) High magnification images showing the evolution of fracture and failure caused by MEMS applied tensile stress (scale bar: 60 nm). (e) Experimental true stress–strain data measured on the GO nanosheet.

actuation voltage increment of 0.5 V. As the tensile test progressed, failure initiated at the interface connecting two sides of the GO nanosheet, where amorphous carbon was deposited. This indicates that pristine GO nanosheet has higher strength than that of amorphous carbon. Crack propagated along the width of the amorphous carbon with a larger and larger opening. Finally a catastrophic failure occurred at a strain of ~4%. Comparing the fracture surface of amorphous carbon with that before carbon linking, it is obvious that major failure occurred to the amorphous carbon but not the GO nanosheet. The stress–strain response (stress reported in true stress) (figure 4(e)) reveals that the carbon linked GO nanosheet has a failure strength of 4.4 ± 2.2 GPa, which is lower than that of pristine GO nanosheet [10] and theoretically predicted amorphous carbon [15].

Conclusion

A pre-fractured GO nanosheet was linked by amorphous carbon via electron beam induced deposition on a monolithic MEMS device under TEM imaging. On-chip tensile testing was performed on the carbon linked GO nanosheet. The results show that the carbon linked GO nanosheet has a strength in the gigapascal range, which is near the lower range of that of a pristine GO nanosheet [10] and theoretically predicted strength for amorphous carbon [15]. The TEM compatibility of the monolithic MEMS device enables simultaneous mechanical measurement and advanced TEM characterization of 2D nanomaterials.

Acknowledgments

The authors acknowledge funding by the Natural Sciences and Engineering Research Council of Canada (NSERC) through Discovery Grants to TF and YS. YS also acknowledges financial support of an Ontario Research Fund —Research Excellence Grant. MEMS fabrication technical support was provided by CMC Microsystem. The authors thank Dr Stas Dogel for design of the TEM holder and Charles Soong (Hitachi High Tech, Canada) and Sal Boccia (Ontario Centre for the Characterization of Advanced Materials) for technical assistance and discussion. The authors also thank Toronto Nanofabrication Center for fabrication support.

References

[1] Coleman J N, Khan U and Gun'ko Y K 2006 *Adv. Mater.* **18** 689
[2] Eda G and Chhowalla M 2009 *Nano Lett.* **9** 814
[3] Kim K S, Zhao Y, Jang H, Lee S Y, Kim J M, Ahn J H, Kim P, Choi J Y and Hong B H 2009 *Nature* **457** 706
[4] Lee J K, Smith K B, Hayner C M and Kung H H 2010 *Chem. Commun. (Camb)* **46** 2025
[5] Li X *et al* 2012 *Adv. Funct. Mater.* **22** 1647
[6] Lee G-H *et al* 2013 *Science* **340** 1073
[7] Cao C, Daly M, Singh C V, Sun Y and Filleter T 2015 *Carbon* **81** 497
[8] Zhang Y, Liu X Y, Ru C H, Zhang Y L, Dong L X and Sun Y 2011 *J. Microelectromech. Syst.* **20** 959
[9] Dongfeng Z, Breguet J M, Clavel R, Sivakov V, Christiansen S and Michler J 2010 *J. Microelectromech. Syst.* **19** 663
[10] Cao C, Daly M, Chen B, Howe J Y, Singh C V, Filleter T and Sun Y 2015 *Nano Lett.* **15** 6528
[11] Cao C, Sun Y and Filleter T 2014 *J. Mater. Res.* **29** 338
[12] Filleter T, Bernal R, Li S and Espinosa H D 2011 *Adv. Mater.* **23** 2855
[13] Changhong C, Chen B, Filleter T and Yu S 2015 *28th IEEE Int. Conf. on Micro Electro Mechanical Systems (MEMS) 2015* unpublished
[14] Egerton R 2011 *Electron Energy-Loss Spectroscopy in the Electron Microscope* (New York: Springer)
[15] Remediakis I N, Fyta M G, Mathioudakis C, Kopidakis G and Kelires P C 2007 *Diam. Relat. Mater.* **16** 1835